

Design Novel Fuzzy Logic Controller of IPMSM for Electric Vehicles

Wu Huangyuan¹, Wang Shuanghong¹, Shao Keran¹, Jianbo Sun¹

¹State Key Laboratory of Advanced Electromagnetic Engineering and Technology, Huazhong University of Science and Technology, Wuhan 430074, Hubei Province, China
whynot1006@163.com

Abstract—This paper presents a novel fuzzy logic controller (FLC) for an interior permanent magnet synchronous motor (IPMSM) in electric vehicles (EV). As an IPMSM used for electric vehicles, d - and q -axis inductances are varied in wide range. Thus, based on inductances variation, the inductances are analysed as a function of both current magnitude and phase. Then, a novel fuzzy logic control algorithm is proposed that uses the parameters variation of the inductances is proposed. The algorithm adjusts the reference current of the drive system according to the speed and torque statuses. A digital signal processor (DSP) chip TMS28335 is used to implement a complete drive system for a 50kW IPMSM prototype motor. Experimental results have been carried out in order to prove the effectiveness of the new FLC.

Index Terms—FLC, IPMSM, flux weakening, varied inductances.

I. INTRODUCTION

The permanent magnets of the interior permanent magnet synchronous motor (IPMSM) are buried in the rotor core. Due to this kind of geometry, IPMSM has a robust mechanical structure, a low effective air gap, and a rotor saliency [1]. These features allow the IPMSM could run both in constant torque region with greater torque output capability and constant power region with wider speed range. Wide speed range is strongly required in many industry applications such as electric vehicle, spindle drives and so on. In a permanent magnet motor, it is not possible to control directly the magnet flux. The air-gap flux, however, is weakened by the demagnetizing current in the direct axis; this control method is called flux-weakening.

All previous studies based the control algorithm for the IPMSM drive system on accurate parameter model. However, generally, all of the parameters of the IPMSM are varied as the temperature change. Furthermore, due to the core saturation, the inductances varied depending on the load condition and current phase [2]–[5]. The FEM (finite element modelling) and the experiments were used to analyse the nonlinearly characteristic of the inductances [6]. In [7], the new material and new structure IPMSM were developed to reduce the influence of core saturation.

So far, in order to improve the performance in the

constant power region, many literatures have discussed how to process the varied inductance on the influence of the current trajectory in real time [8]–[12]. In recent years, researchers have tried to apply the intelligent controller in the

IPMSM drives [13]–[18]. It is advantageous that the intelligent controllers do not demand an accurate mathematical model of the system. Theoretically, they can handle any nonlinear model for the control system.

The look up table method was used to improve the performance with an adaptive controller, but this method need lots of off line experiments, and the controller is not suitable for program transplantation. In [19], the authors developed a on line parameters estimation scheme, however, the scheme only have good performance in the steady state, and the characteristics of the electric vehicle drive system is dynamic in the most time. Reference [20] presented a neural controller for an EV drive system in real time, however, in that study the controller was a complicated one and with high computational burden.

Compared to many types of intelligent controllers, FLC is the one of the most easy to implement for high performance IPMSM drive [21]–[23]. A novel FLC algorithm has been proposed in [21], however, the variations of the parameters are not considered. In [22], only the variation of q -axis inductance is considered, this can lead to torque output capacity reduction.

This paper presents a novel FLC in order to obtain an IPMSM drive system with high performances. At first, the parameters variation characteristics are analysed. Then, the d , q current calculation methods and adjust algorithm are incorporated into the controller. At last, the complete drive system and communication system for the EV have been successfully implemented by using DSP chip TMS28335 and dSpace for a prototype 50 Kw motor.

II. MODELLING OF IPMSM

Assuming that the motor has sinusoidal stator excitation, in the d - q reference synchronous coordinate the mathematical model for an IPMSM are given by:

$$u_d = R_s i_d + L_d(i_d, i_q) \frac{di_d}{dt} - \tilde{S} L_q(i_d, i_q) i_q, \quad (1)$$

$$u_q = R_s i_q + L_q (i_d, i_q) \frac{di_q}{dt} + \check{S} L_d (i_d, i_q) i_d + \check{S} \mathcal{E}_f, \quad (2)$$

$$T_{em} = \frac{3}{2} p_n [\mathcal{E}_f i_q + (L_d (i_d, i_q) - L_q (i_d, i_q) i_d i_q)], \quad (3)$$

$$T_{em} = T_L + B \dot{\theta}_r + J \frac{d\dot{\theta}_r}{dt}, \quad (4)$$

where \mathcal{E}_f is flux linkage of permanent magnet excitation, L_d and L_q are the related d - q -axis inductance, respectively, i_d and i_q are d - q -axis current, u_d and u_q are d - q -axis stator voltage, R_s is the stator resistance, and $\dot{\theta}_r$ are the electrical and mechanical angular velocity. p_n are the poles pairs of the motor, T_L is the load torque, B and J are viscous friction and rotor inertia coefficient. Because of the reluctance torque, the electrical torque T_{em} is nonlinear.

The maximum voltage of the system V_{max} which the inverter can provide to the motor is limited by battery voltage of the EV. In addition the limiting current i_{lim} depends on battery rating and machine thermal rating. Accordingly, the voltage and current of the system must meet the equation:

$$\sqrt{u_d^2 + u_q^2} \leq V_{max}, \quad (5)$$

$$\sqrt{i_d^2 + i_q^2} \leq i_{lim}. \quad (6)$$

The amplitude of the impressed stator vector current i_s can be expressed with the d - q -axis current and the voltage can be expressed by the battery as it follows:

$$\sqrt{i_d^2 + i_q^2} = i_s, \quad (7)$$

$$V_{max} = u_{dc} / \sqrt{3}. \quad (8)$$

III. DESIGN OF FLC

A. The System Block Diagram

Figure 1 shows the block diagram of the control strategy of the IPMSM drive system. In current studies, the entire operating range consists of two typical regions, generally, below the rated speed region is called constant torque region, while above the rated speed is called constant power region.

As the rotor speed is the basis that decides determines the operating region the motor, rotor speed must be considered as an input signal for the FLC. The effect of the speed error is to be able to follow the command speed, whereas the acceleration input is to make the process more stable. Therefore, the rotor speed, speed error and acceleration are the inputs of the FLC. Respectively, the d - q -axis currents are selected as the outputs for the FLC to control the torque and flux. The novel FLC proposed in this paper is composed of two parts; the output of the first part is the unregulated q -

axis current i_{qc} , while the second part will regulate the i_d and i_q according to the magnitude of i_{qc} and the rotor speed. The analysis have been carried out using the per unit form, the base current value is 250 A, and the base speed is 4000 r/min.

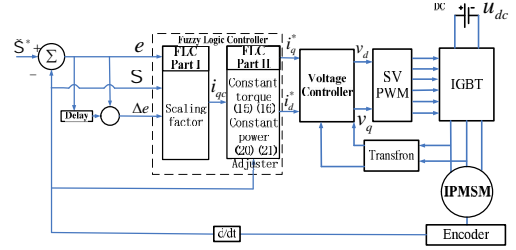


Fig. 1. Block diagram of the proposed control system.

B. Variation Characteristics of Inductances

The studies of the variation characteristics of the L_d and L_q for the prototype motor have been conducted through finite element analysis in Fig. 2. If the variations of the inductances are only considered as a function of current amplitude, the result is similar to the ones of existing literatures that ignores the variation of L_d . However, in the full operation region; the L_d and L_q are varied according to the amplitude and phase of the current.

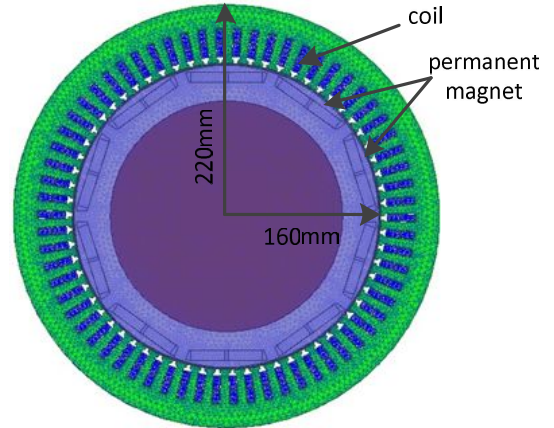
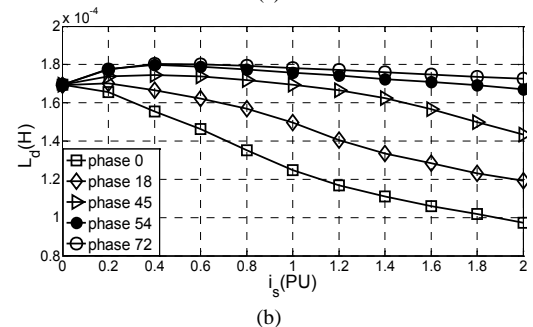
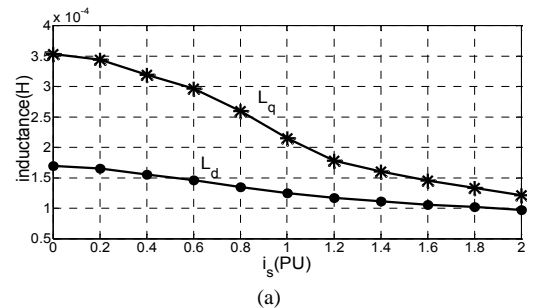


Fig. 2. 2-D mesh model of the IPMSM.



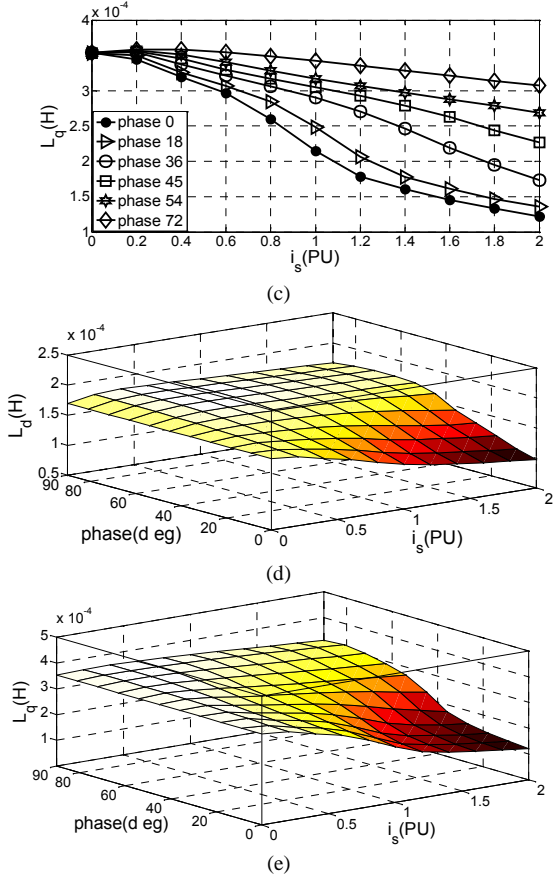


Fig. 3. Variation of inductances by current magnitude and current phase: (a) Inductances characteristics with constant phase 0; (b) Parameters variation of L_d (two-dimension); (c) Parameters variation of L_q (two-dimension); (d) Parameters variation of L_d (three-dimension); (e) Parameters variation of L_q (three-dimension).

It is shown in Fig. 3 that the L_q is much more varied than L_d if the system does not consider current phase, it is important that the L_d is far from a correct value. The research shows that the variation of L_d has a greater impact on the performance of the control system [23]. Therefore it is necessary that the variations of L_d and L_q is a function of both current amplitude and phase in the control system.

C. Control Strategy for Constant Torque Region

Because there is a saliency in IPM motor, so it is necessary to utilize the reluctance torque properly. The armature current vector is controlled according to the maximum torque per ampere (MTPA) operation. Conventionally, the d - and q -axis components of the current vector for the MTPA mode are derived as

$$i_d = \frac{-\mathfrak{E}_f}{2(L_d - L_q)} - \sqrt{\frac{\mathfrak{E}_f^2}{4(L_d - L_q)^2} + i_q^2}. \quad (9)$$

It is shown in Fig. 4, the currents will track the locus as the load increasing, with the rated load, the vector current will reach the rated limit point R. If the motor parameters are constant with rated value, considering the overload status, then the MTPA trajectory is \overline{ORM} . However, it has been analysed that the inductances are both changed according to the current amplitude and the phase, and the actual MTPA control curve is \overline{ORN} . As the load increases, especially in

the overload status, the current curve with the constant parameters will be far away from the actual current trajectory. In the constant torque region, the presented control strategy is based on the variation characteristics of L_d and L_q . Figure 4 illustrates that although the d - q axis inductances are both changed, under the rated current condition the saliency of the prototype motor increases as the current increases. Moreover decreases as current increases in the overload status. The MTPA curves moves close to the q axis with decrease of the saliency and move far with increase of the saliency. Thus, the strategy in the constant region could be determined. At first, the MTPA curve with rated parameters can be selected as the base curve, then, using the part II of FLC to adjust the reference current on the basis of the magnitude of the current.

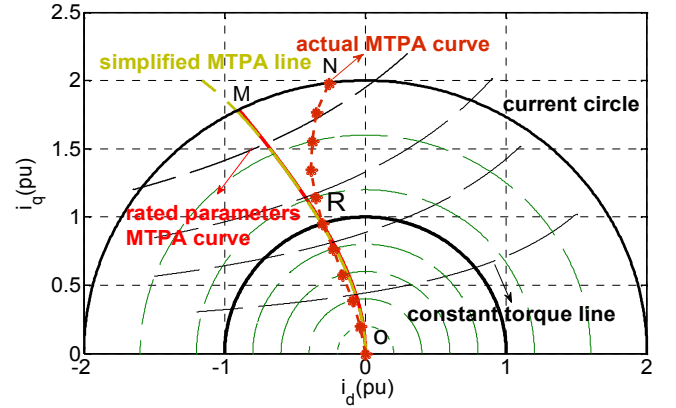


Fig. 4. Current curve in the constant torque region.

When the FLC applies to microprocessor chips, the use of exact MTPA equation (9) to design a FLC is not easy. Using the Maclaurin series, the equation can be simplified

$$i_d = \frac{(L_d - L_q)}{\mathfrak{E}_f} i_q^2 - \frac{(L_d - L_q)^3}{\mathfrak{E}_f^3} i_q^4 - \dots \quad (10)$$

According to parameters of Table I, it is observed that the $(L_q - L_d)/\mathfrak{E}_f \ll 1$, above the fourth order of i_q , the sum is only 0.3 % of the total polynomial, Hence, the reference currents in the MTPA region are

$$i_d = \frac{(L_d - L_q)}{\mathfrak{E}_f} i_q^2. \quad (11)$$

Figure 4 shows that the simplified MTPA curve could match the original curve very well. It could greatly reduce the computational burden. In the constant torque region, the basis equations of the FLC are:

$$i_{qc} = f_{\text{Fuzzy}}(e, \dot{S}, \Delta e), \quad (12)$$

$$\Delta i_{qt} = f_{\text{Fuzzy}}(i_{qc}), \quad (13)$$

$$\Delta i_{dt} = f_{\text{Fuzzy}}(i_{qc}), \quad (14)$$

$$i_q^* = i_{qc} + \Delta i_{qt}, \quad (15)$$

$$i_d^* = \frac{(L_d - L_q)}{\mathfrak{E}_f} i_{qc}^2 + \Delta i_{dt}. \quad (16)$$

D. Control Strategy for Constant Power Region

In high-speed region of the IPMSM, the speed constrained by back electromotive force. Without appropriate flux weakening scheme, the controller could be saturated or even lose its controllability. As shown in Fig. 5, in the constant power region, the running area is bounded by the current limit curve, voltage constraint curve and d -axis line. The relationship between the d - q axis current in constant power region contain current and voltage constraints is

$$i_d = -\frac{\mathcal{E}_f}{L_d} + \frac{1}{L_d} \sqrt{\frac{U_{\max}^2}{\tilde{S}^2} - (L_q i_q)^2}. \quad (17)$$

As aforementioned, the parameters of motor varied according to the magnet and the phase of the current, without properly adjusting the current, the performance of the control system could get worse because of the varied parameters. As show in Fig. 5, similarly to the method in the constant torque region, select the rated parameter current curve as a base trajectory, then adjust the d - q axis current basing on the trajectory. With speed increasing, the current trajectory will move close to d -axis, it also means the current phase becomes larger. So the rotor speed could regard as the phase angle information of the current. It is hardly to use an equation to describe the relationship between the current deviation and current amplitude or phase. The FLC simplifies the expression, as seen in Fig. 5, the current deviation $EF > MN$, $PS > MN$, so the basic rule of the FLC could be ascertained: if the current is larger, then the deviation is greater, if the speed is higher, then the deviation is bigger.

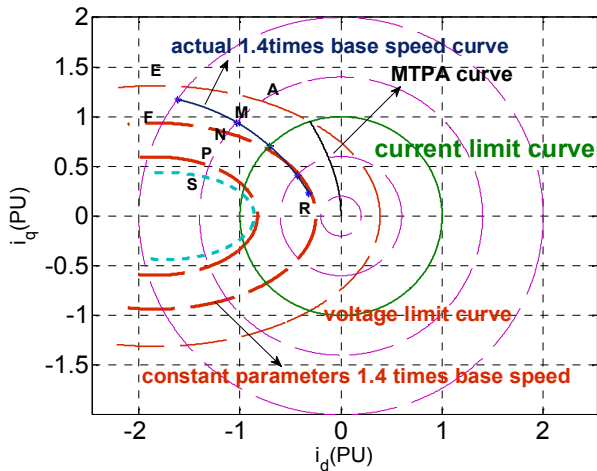


Fig. 5. Current curve in the constant power region.

TABLE I. THE PARAMETER AT RATED CONDITION.

Parameter	Value
\mathcal{E}_f/Wb	0.0753
L_q/mH	0.277
L_d/mH	0.164
R_s/Ω	0.007
i_{lim}/A	250
u_{dc}/V	336
Poles	5
Rated Speed/(r/min)	4000

In order to simplify the FLC, the equation should be rewritten. Reasonable assuming $\tilde{S}_c f = V_{\max}$. Then, write the

electrical angular velocity as per unit calculation: $\tilde{S}_{pu} = \tilde{S}/\tilde{S}_c$, using Maclaurin series expansion to simplify the polynomial, then the basic equation of the constant power region expressions are:

$$\Delta i_{qf} = f_{\text{Fuzzy}q}(\tilde{S}, i_{qc}), \quad (18)$$

$$\Delta i_{df} = f_{\text{Fuzzy}d}(\tilde{S}, i_{qc}), \quad (19)$$

$$i_q^* = i_{qc} + \Delta i_{qf}, \quad (20)$$

$$i_d^* = -\frac{\mathcal{E}_f}{L_d} + \frac{\mathcal{E}_f}{L_d \tilde{S}_{pu}} - \frac{L_q}{L_d} \frac{L_q \tilde{S}_{pu}}{2\mathcal{E}_f} i_{qc}^2 + \Delta i_{df}. \quad (21)$$

IV. FUZZY LOGIC RULES

Once the basic equation is determined, then the fuzzy control rules for the system can be deduced. The controller is divided into two parts, the scaling factors (k_s , k_e , $k_{\Delta e}$) in part I and the (k_s , k_{iqc}) in part II have been chosen by the trial-and-error method. The main rules in part are show in Table II.

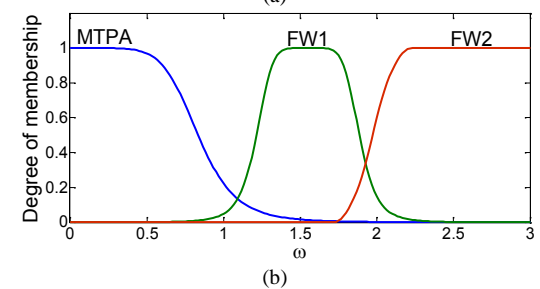
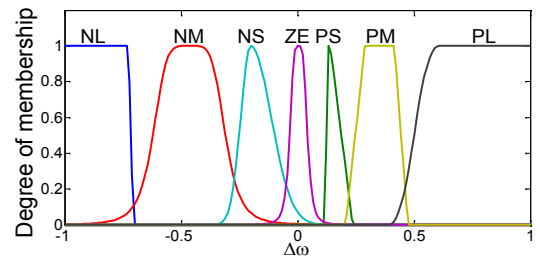
TABLE . THE MAIN RULES IN PART .

e	i_{qc}
PL (positive large)	PL (positive large)
PM (positive middle)	PM (positive middle)
PS (positive small)	PS (positive small)
ZE (zero)	NC (not changed)
NL (negative large)	NL (negative large)
NM (negative middle)	NM (negative middle)
NS (negative small)	NS (negative small)

Assuming $\Delta \tilde{S} = \tilde{S} - \tilde{S}_{\text{rate}}$, it is utilized to determine which region the motor is running in, accordingly, the main rules used in part II for FLC are show in Table III.

TABLE I. THE MAIN RULES IN PART .

	If	Then	
	i_{qc}	i_{df}	i_{qf}
PS	L (large)	NL	NL
PS	M (middle)	NM	NM
PS	S (small)	NS	NS
PM	L (large)	NL	NL
PM	M (middle)	NM	NM
PM	S (small)	NS	NS
PL	L (large)	NL	NL



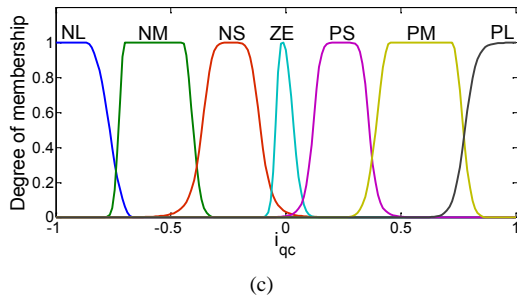


Fig. 6. Membership of the main controlled variable: (a) Membership functions for speed error \dot{S} ; (b) Membership functions for speed error \dot{S} ; (c) Membership functions for i_{qc} .

Figure 6 shows the membership functions of the main input–output variables for the FLC.

V. PERFORMANCE INVESTIGATION

The advantages of the proposed FLC have been researched through experiment tests. The complete hardware drive system has been implemented by DSP TMS28335 for a prototype 50 kW motor. The test motor and the prototype EV are both manufactured by the Dongfeng Company. The experimental setup and the EV used for the experiments are shown in Fig. 8. EV communicates using the standard CAN bus. The sampling frequency for both speed and current is 20 kHz. Sample results have been transmitted to the dSpace controller through the CAN bus which is the standard communication of the EV. The experimental waveform data are provided by dSpace.

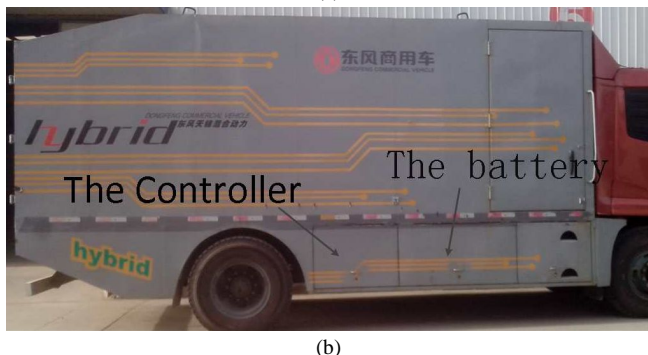
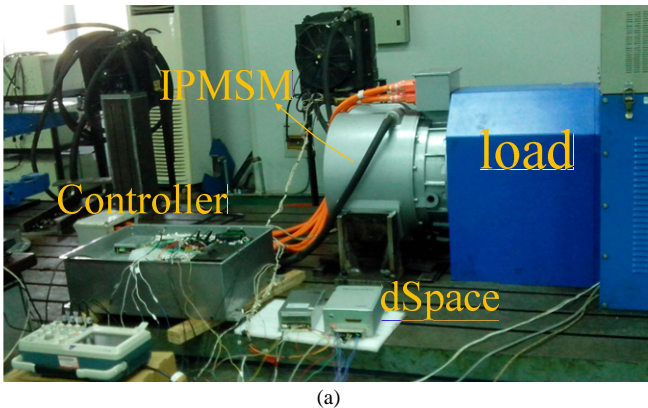


Fig. 7. Experimental setup for the proposed FLC-based IPMSM drive: (a) Experimental equipment; (b) The Prototype EV.

The performances between the conventional FLC which not considered the variation inductance and proposed FLC have made a detailed comparison. In the constant torque region, the command speed for IPMSM system is a step

command of 3600r/min with load 60N·m respectively for the two types FLC. Compared to the conventional FLC, Fig. 8 gives a comparison between conventional FLC and the proposed method, which appears more efficient. In fact, the proposed FLC could achieve the target speed in lower time, moreover, it also demands a lower stator current which shows in Fig. 8(d). This is benefit from the current adjuster in part II of the FLC. Thus, the copper losses of the system could be minimized, and accordingly, the efficiency of the system will be maximized.

To show the performances in the constant power region the command speed changes to 7000 r/min with the load maintained 60 Nm in Fig. 9. The drive system still behaves well as in the constant torque region; also, the proposed FLC has a better dynamic performance and efficiency in the constant power region.

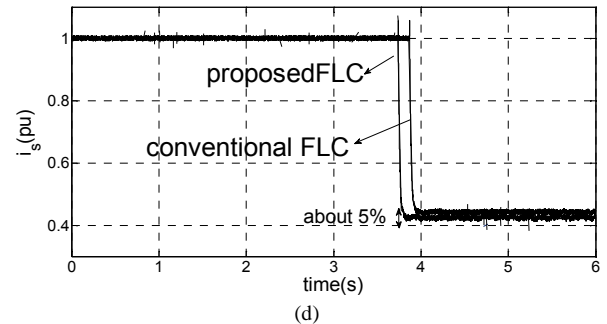
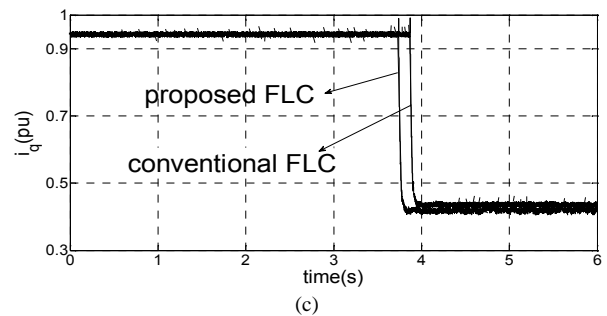
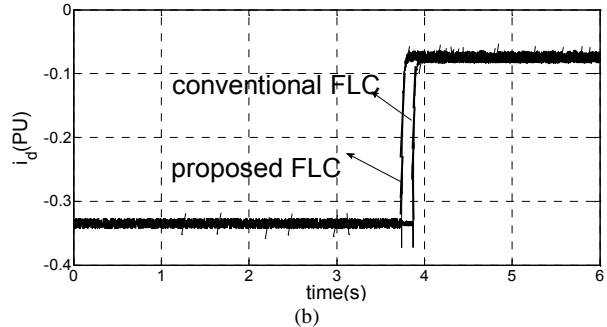
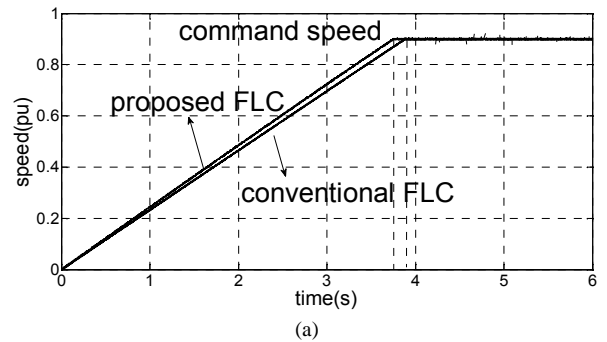


Fig. 8. Comparison of the speed and current response in the Constant torque region: (a) The Prototype EV Comparison of the speed response; (b) Comparison of the i_d ; (c) Comparison of the i_q ; (d) Comparison of the i_s .

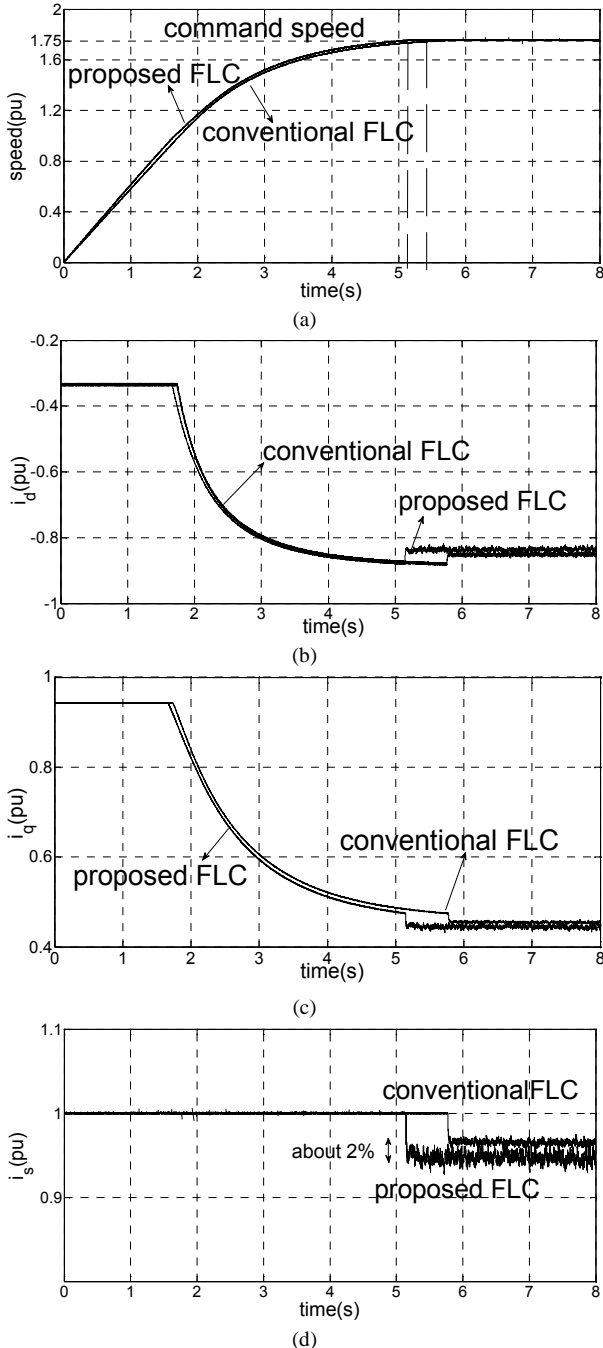


Fig. 9. Comparison of the speed and current response in the Constant power region: (a) Comparison of the speed response; (b) Comparison of i_d ; (c) Comparison of i_q ; (d) Comparison of i_s .

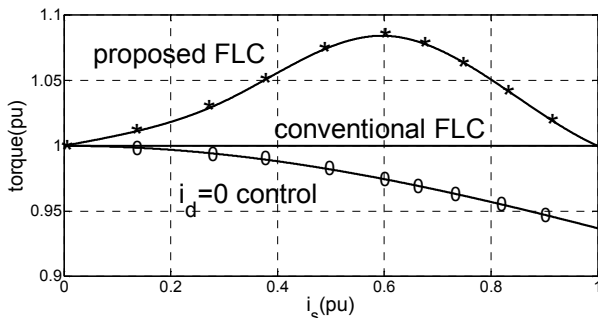


Fig. 10. Torque output curve comparison in the constant torque region.

In addition, this paper has compared the experimental results for three control methods which are the field-orientated controller in the constant torque region,

conventional FLC and the novel FLC which this paper proposed. Use the output torque of the conventional FLC as a basic value.

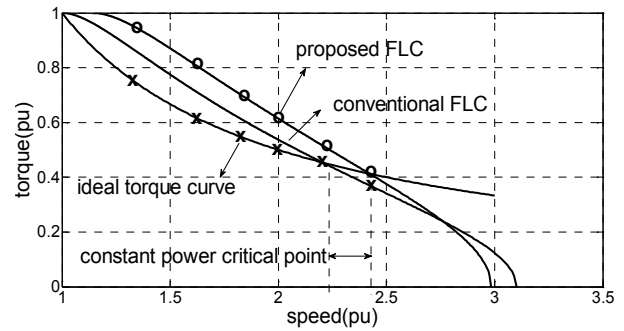


Fig. 11. Torque output curve comparison in the constant power region.

From Fig. 10, it is obviously the proposed FLC has a better torque output capacity. A further comparison between the two types FLC in the constant power region is shown in Fig. 11. The figures show that the proposed controller has a wider constant power range than the old one.

VI. CONCLUSIONS

In this paper, the variation characteristics of the inductances are analysed, then, a novel fuzzy logic controller for the IPMSM drive system is proposed which is suitable for the high saliency IPMSM. The proposed FLC model simplifies control both in the constant torque region and the constant power region. The experimental device for the IPMSM drive system and the test EV are completely implemented, using the DSP TMS28335 for a prototype 50 kW motor.

The performances between the conventional FLC and the novel FLC proposed in this paper have been compared through the experimental tests. As compared to the conventional FLC, the novel FLC has a faster speed response characteristic in the full operation region. The experiments show that the novel FLC can provide a better torque output capacity in the constant torque region, simultaneously, it can extend the operating speed limit in the constant power region. Moreover, the novel FLC reduced the copper loss because of the current adjuster. The superiority and the effectiveness of the proposed scheme have been proved by the experimental results.

REFERENCES

- [1] P. Zhou, Di. Lin, G. Wimmer, N. Lambert, Z. J. Cendes, "Determination of d - q axis parameters of interior permanent magnet machine", *IEEE Trans. Magnetics*, vol. 2, pp. 3125–3128, 2010. [Online]. Available: <http://dx.doi.org/10.1109/TMAG.2010.2043507>
- [2] R. Dutta, M. F. Rahman, "A comparative analysis of two test methods of measuring d - and q -axes inductances of interior permanent magnet machine", *IEEE Trans. Magnetics*, vol. 42, pp. 3712–3718, 2006. [Online]. Available: <http://dx.doi.org/10.1109/TMAG.2006.880994>
- [3] Kou Baoquan, Cheng Shukan, "Flux-weakening-characteristic analysis of a new permanent-magnet synchronous motor used for electric vehicles", *IEEE Trans. plasma science*, vol. 39, no. 1, 2011. [Online]. Available: <http://dx.doi.org/10.1109/TPS.2010.2076355>
- [4] Inoue Yu, Kawaguchi Ye, "Performance improvement of senseless IPMSM drives in a low-speed region using online parameter identification", *IEEE Trans. Industry Applications*, vol. 47, no. 2,

- pp. 798–804, 2012.
- [5] M. A. Rahman, R. M. Milasi, C. Lucas, “Implementation of emotional controller for interior permanent-magnet synchronous motor drive”, *IEEE Trans. Industry Applications*, vol. 44, no. 5, pp. 1466–1476, 2008. [Online]. Available: <http://dx.doi.org/10.1109/TIA.2008.2002206>
- [6] Sung-Yoon Jung, Jinseok Hong, “Current minimizing torque control of the IPMSM using Ferrari’s method”, *IEEE Trans. Power Electronic*, vol. 28, no. 12 pp. 5603–5617, 2014. [Online]. Available: <http://dx.doi.org/10.1109/TPEL.2013.2245920>
- [7] Shiyang Duan, Libin Zhou, “Flux weakening mechanism of interior permanent magnet synchronous machines with segmented permanent magnets”, *IEEE Trans. applied superconductivity*, vol. 24, no. 3 pp. 105–110, 2014.
- [8] M. N. Uddin, M. N. Chy, “A novel fuzzy logic controller base torque and flux controls of IPM Synchronous motor”, *IEEE Trans. Industry Applications*, vol. 43, no. 6, pp. 1220–1229, 2010. [Online]. Available: <http://dx.doi.org/10.1109/TIA.2010.2045334>
- [9] Cheol Jo, Seol Ji-Yun, Ha In-Joong, “Flux-weakening control of IPM motors with significant effect of magnetic saturation and stator resistance”, *IEEE Trans. Industry Electronics*, vol. 55, no. 3, pp. 1330–1340, 2008. [Online]. Available: <http://dx.doi.org/10.1109/TIE.2007.910524>
- [10] M. S. Hossain, M. J. Hossain, “Performance analysis of a novel fuzzy logic and MTPA based speed control for IPMSM drive with variable d- and q-axis inductances”, in *Proc. 12th Int. Conf. Computers and Information Technology*, Dhaka, 2009, pp. 361–366
- [11] Y. S. Jeong, J. Y. Lee, “Adaptive flux observer with on-line inductance estimation of an IPM synchronous machine considering magnetic saturation”, *Journal of Power Electronics*, vol. 9, pp. 188–197, 2009.
- [12] T. S. Kwon, G. Y. Choi, M. S. Kwak, “Novel flux- weakening control of an IPMSM for Quasi-six-step operation”, *IEEE Trans. Industry Applications*, vol. 44, pp. 1722–1731, 2008. [Online]. Available: <http://dx.doi.org/10.1109/TIA.2008.2006305>
- [13] J. W. Park, D. H. Koo, J. M. Kim, “Improvement of control characteristics of interior permanent-magnet synchronous motor for electric vehicle”, *IEEE Trans. Industry Applications*, vol. 37, no. 6, pp. 1754–1760, 2010. [Online]. Available: <http://dx.doi.org/10.1109/28.968188>
- [14] Wu Huangyuan, Wang Shuanghong, “Simplified fuzzy logic based flux weakening speed control of IPMSM drive”, in *Proc. 2011 Int. Conf. Electrical Machines and Systems*, Beijing, 2011, pp. 1272–1275.
- [15] A. Khlaief, M. Bendjedia, M. Boussak, M. Gossa, “A nonlinear observer for high-performance sensorless speed control of IPMSM drive”, *IEEE Trans. Power Electronics*, vol. 38, pp. 3028–3040, 2012. [Online]. Available: <http://dx.doi.org/10.1109/TPEL.2011.2175251>
- [16] N. Ozturk, “Speed control for DC motor drive based on fuzzy and genetic PI controller – a comparative study”, *Elektronika ir Elektrotechnika*, vol. 123, pp. 44–48, 2012.
- [17] M. N. Uddin, M. Azizur Rahman, “High-speed control of IPMSM drives using improved fuzzy logic algorithms”, *IEEE Trans. Industrial Electronics*, vol. 54, pp. 190–199, 2007. [Online]. Available: <http://dx.doi.org/10.1109/TIE.2006.888781>
- [18] Sung-Yoon Jung, Jinseok Hong, Kwanghee Nam, “Current minimizing torque control of the IPMSM using Ferrari’s method”, *IEEE Trans. Industry Applications*, vol. 28, pp. 5603–5617, 2012.
- [19] Jo Cheol, Seol Ji-Yun, Ha In-Joong, “Flux-weakening control of IPM motors with significant effect of magnetic saturation and stator resistance”, *IEEE Trans. Industrial Electronics*, vol. 55, pp. 1330–1340, 2008. [Online]. Available: <http://dx.doi.org/10.1109/TIE.2007.910524>
- [20] A. Taheri, “Efficiency optimization of six-phase induction motors by fuzzy controller”, *Elektronika ir Elektrotechnika*, vol. 19, pp. 49–52, 2013.
- [21] Han Ho Choi, Nga Thi-Thuy Vu, Jin-Woo Jung, “Digital implementation of an adaptive speed regulator for a PMSM”, *IEEE Trans. Power Electronics*, vol. 6, pp. 3–8, 2011. [Online]. Available: <http://dx.doi.org/10.1109/TPEL.2010.2055890>
- [22] Y.A.-R.I. Mohamed, T. K. Lee, “Adaptive self-tuning MTPA vector controller for IPMSM drive system”, *IEEE Trans. Energy Conversion*, vol. 21, pp. 636–644, 2006. [Online]. Available: <http://dx.doi.org/10.1109/TEC.2006.878243>
- [23] Chen Yangsheng, Huang Bixia, Zhu Ziqiang, “Influence of inaccuracies in machine parameters on field-weakening performance of PM brushless AC drives”, in *Proc. CSEE*, vol. 28, pp. 92–98, 2008.